VIII ECCOMAS Thematic Conference on Smart Structures and Materials
SMART 2017
A. Güemes, A. Benjeddou, J. Rodellar and J. Leng (Eds)

# ADVANCED VIBRATION CONTROL OF LARGE STRUCTURES WITH DISTRIBUTED MULTI-ACTUATOR SYSTEM AND PARTIAL STATE INFORMATION

**F. PALACIOS-QUIÑONERO*, J. RUBIÓ-MASSEGÚ*, J.M. ROSSELL* AND J. RODELLAR†**

*Universitat Politècnica de Catalunya (UPC)
Department of Mathematics
EPSEM. Av. Bases de Manresa 61-73, 08242 Manresa, Spain
e-mail: {francisco.palacios, josep.rubio, josep.maria.rossell}@upc.edu

† Universitat Politècnica de Catalunya (UPC)
Department of Mathematics
EEBE. C. Eduard Maristany 10-14, 08019 Barcelona, Spain
e-mail: jose.rodellar@upc.edu

**Key words:** Structural vibration control, Output-feedback control, Multi-actuator systems, Seismic protection

**Abstract.** In this paper, the design and performance of partial-state controllers with incomplete multi-actuation systems for the seismic protection of tall buildings is investigated. The proposed approach considers a partially instrumented multi-story building with an incomplete system of interstory force-actuation devices implemented at selected levels of the building, and an associated set of collocated sensors that measure the interstory drifts and velocities corresponding to the instrumented stories. The main elements of the proposed controller design methodology are presented by means of a twenty-story building with two different actuation schemes. For these control configurations, partial-state controllers are designed following a static output-feedback $H_\infty$ controller design approach, and the corresponding frequency and time responses are investigated. The obtained results clearly indicate that the proposed partial-state controllers are effective in mitigating the building seismic response. They also show up that a suitable distribution of the instrumented stories is a relevant factor in the control system design.

## 1 INTRODUCTION

Protection of large buildings and civil structures against the damaging effects of seismic excitations is an important issue that has attracted increasing research attention over the last years. In some advanced approaches, complex and sophisticated vibration control systems are considered. These control configurations involve a large set of sensors and actuation devices, which are widely distributed throughout the structure, and work coordinately to mitigate the structure vibrational response [1, 2]. Overall, the controlled structure can be seen as a huge mechatronic system, which is able to produce an intelligent reaction to mitigate the negative effects of external disturbances. In this work, we present a controller design methodology for the seismic protection of tall buildings equipped with a distributed set of actuators and sensors. More specifically, we assume that some of the building stories are equipped with an interstory force-actuation device and a sensing unit that can measure the corresponding interstory drift and velocity [3]. We also assume that the building is only partially instrumented and, consequently, the available state information is incomplete. Using a distributed set of small actuation devices instead of a single large actuator allows reducing the structural loads produced by the control system, and helps to provide a more balanced control action. A distributed set of collocated sensors is a natural and technically convenient choice. Additionally, considering a partially instrumented scheme is a realistic approach for tall buildings with a large number of stories. It should be noted that, in this context, the control system design comprises two different problems: (1) computing an effective controller for a given distribution of the instrumented stories (controller design), and (2) determining an optimal distribution of the instrumented stories (optimal control configuration). Obviously, a computationally efficient solution to the first problem can help to explore the effectiveness of different control configurations and, consequently, can contribute to obtain an optimal solution to the second problem. Due to the high dimensionality and information constraints, the considered controller design problem leads to serious issues, both theoretical and computational. The solution proposed in this work is based on an output-feedback $H_\infty$ approach, and allows obtaining effective controllers with incomplete state information by solving a two-step Linear Matrix Inequality (LMI) optimization problem [4]. The main results are presented by means of a twenty-story building with two different actuation schemes. The obtained results confirm the effectiveness of structural vibration control strategies with incomplete multi-actuator systems and partial state information. They also point out that an enhanced performance can be achieved by a suitable distribution of the instrumented stories.

The rest of the paper is organized as follows: In Section 2, a state-space model for the twenty-story building with incomplete actuation schemes is presented. In Section 3, full-state and partial-state controllers are designed for the different control configurations and the corresponding frequency characteristics are investigated. In Section 4, numerical simulations of the time responses are conducted and illustrative peak-value plots of the interstory drifts, story absolute accelerations and control efforts are presented and compared. Finally, in Section 5, some conclusions and future research directions are briefly discussed.

## 2 BUILDING MODEL

Let us consider an $n$-story building whose lateral displacement can be described by the second-order differential equation

$$M\,\ddot{q}(t) + C_d\,\dot{q}(t) + K_s\,q(t) = T_u u(t) + T_w w(t), \tag{1}$$

where $q(t) = \left[q_1(t), \ldots, q_n(t)\right]^T$ is the vector of story displacements with respect to the ground, $w(t)$ is the seismic ground acceleration and $u(t)$ is the vector of control actions. $M$, $C_d$ and $K_s$ are the mass, damping and stiffness matrix, respectively, which model the mechanical characteristics of the building, $T_u$ is the control location matrix and $T_w$ is the disturbance input matrix. The

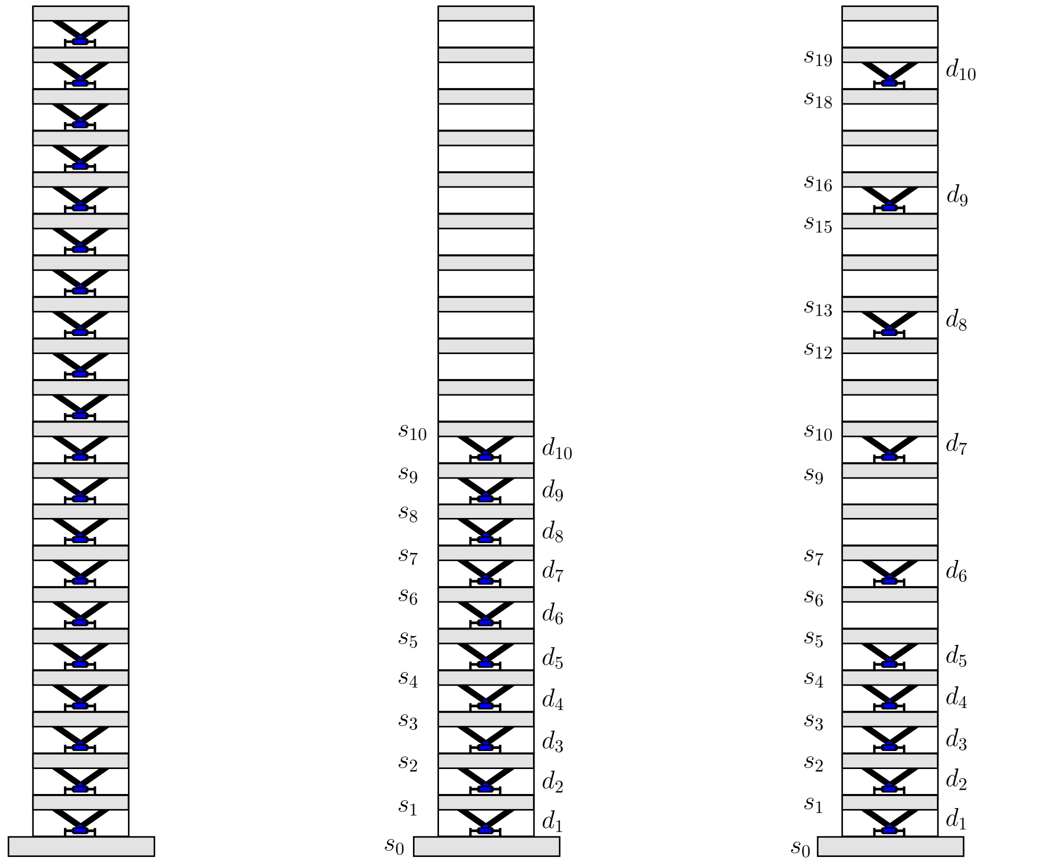


(a) Complete actuation scheme (b) Partial actuation scheme 1 (c) Partial actuation scheme 2

**Figure 1**: Interstory actuation schemes. (a) Complete actuation scheme. (b) Partial actuation scheme AS1, with $m = 10$ actuators located at positions $P_1 = [1, 2, \ldots, 10]$. (c) Partial actuation scheme AS2, with $m = 10$ actuators located at positions $P_2 = [1, 2, 3, 4, 5, 7, 10, 13, 16, 19]$.

mass matrix is a diagonal matrix $M = \mathrm{diag}(m_1, m_2, \ldots, m_n)$, and the stiffness matrix has the following tridiagonal structure:

$$K_s = \begin{bmatrix} k_1+k_2 & -k_2 & & & & \\ -k_2 & k_2+k_3 & -k_3 & & & \\ & \cdots & \cdots & \cdots & & \\ & & \cdots & \cdots & \cdots & \\ & & & -k_{n-1} & k_{n-1}+k_n & -k_n \\ & & & & -k_n & k_n \end{bmatrix}, \qquad (2)$$

where $m_i$ and $k_i$, $i = 1, \ldots, n$, denote the mass and stiffness coefficient of the $i$-th story, respectively. The damping matrix $C_d$ can be computed from $M$ and $K$ by setting a proper damping ratio on the building modes [5]. The disturbance input matrix has the form $T_w = -M[1]_{n\times 1}$, where $[1]_{n\times 1}$ denotes a vector of dimension $n$ with all its entries equal to 1. The structure of the control location matrix depends on the considered actuation scheme. In this work, we assume that the control forces are exerted by a system of $m$ devices $d_1, \ldots, d_m$, where $d_i$ is an interstory actuator implemented at position $p_i$, which produces a force of magnitude $u_i(t)$ on the story number $p_i$ (upper story), and an opposite force of magnitude $-u_i(t)$ on the story number $p_i - 1$ (lower story). An actuation scheme is determined by a list of positions $P = [p_1, \dots, p_m]$. If the actuation scheme is complete, as the one schematically depicted in Fig. 1(a), then the list of positions is $P_c = [1, 2, \dots, n]$ and the corresponding control location matrix is a square matrix of size $n$ with the following upper-diagonal band form:

$$T_u^{P_c} = \begin{bmatrix} 1 & -1 & & & & \\ & 1 & -1 & & & \\ & & \cdots & \cdots & & \\ & & & \cdots & \cdots & \\ & & & & 1 & -1 \\ & & & & & 1 \end{bmatrix}. \tag{3}$$

For an incomplete actuation scheme with a list of positions $P = [p_1, \dots, p_m]$, $m < n$, the corresponding control location matrix $T_u^P$ is a rectangular matrix of size $n \times m$ that can be obtained by extracting the corresponding columns from $T_u^{P_c}$, that is:

$$T_u^P = T_u^{P_c}(1, 2, ..., n; p_1, \dots, p_m). \tag{4}$$

Thus, for the actuation scheme AS1 in Fig. 1(b), the list of positions is $P_1 = [1, 2, \dots, 10]$ and the control location matrix

$$T_u^{P_1} = T_u^{P_c}(1, 2, \dots, 20; 1, 2, \dots, 10) \tag{5}$$

can be obtained by selecting the first 10 columns of $T_u^{P_c}$, which in this case is a square matrix of size 20. For the actuation scheme AS2 in Fig. 1(c), the list of actuator positions is $P_2 = [1, 2, 3, 4, 5, 7, 10, 13, 16, 19]$ and the corresponding control location matrix has the following form:

$$T_u^{P_2} = T_u^{P_c}(1, 2, ..., 20; P_2) = \begin{bmatrix} 1 & -1 & 0 & 0 & 0 & 0 & 0 & 0 & 0 & 0 \\ 0 & 1 & -1 & 0 & 0 & 0 & 0 & 0 & 0 & 0 \\ 0 & 0 & 1 & -1 & 0 & 0 & 0 & 0 & 0 & 0 \\ 0 & 0 & 0 & 1 & -1 & 0 & 0 & 0 & 0 & 0 \\ 0 & 0 & 0 & 0 & 1 & 0 & 0 & 0 & 0 & 0 \\ 0 & 0 & 0 & 0 & 0 & -1 & 0 & 0 & 0 & 0 \\ 0 & 0 & 0 & 0 & 0 & 1 & 0 & 0 & 0 & 0 \\ 0 & 0 & 0 & 0 & 0 & 0 & 0 & 0 & 0 & 0 \\ 0 & 0 & 0 & 0 & 0 & 0 & -1 & 0 & 0 & 0 \\ 0 & 0 & 0 & 0 & 0 & 0 & 1 & 0 & 0 & 0 \\ 0 & 0 & 0 & 0 & 0 & 0 & 0 & 0 & 0 & 0 \\ 0 & 0 & 0 & 0 & 0 & 0 & 0 & -1 & 0 & 0 \\ 0 & 0 & 0 & 0 & 0 & 0 & 0 & 1 & 0 & 0 \\ 0 & 0 & 0 & 0 & 0 & 0 & 0 & 0 & 0 & 0 \\ 0 & 0 & 0 & 0 & 0 & 0 & 0 & 0 & -1 & 0 \\ 0 & 0 & 0 & 0 & 0 & 0 & 0 & 0 & 1 & 0 \\ 0 & 0 & 0 & 0 & 0 & 0 & 0 & 0 & 0 & 0 \\ 0 & 0 & 0 & 0 & 0 & 0 & 0 & 0 & 0 & -1 \\ 0 & 0 & 0 & 0 & 0 & 0 & 0 & 0 & 0 & 1 \\ 0 & 0 & 0 & 0 & 0 & 0 & 0 & 0 & 0 & 0 \end{bmatrix}. \tag{6}$$

The interstory drift $r_i(t)$ is the relative displacement between the consecutive stories located at the building levels $i$ and $i-1$ (denoted as $s_i$ and $s_{i-1}$ in Fig. 1). The vector of interstory drifts $r(t) = [r_1(t), r_2(t), \dots, r_n(t)]^T$ can be computed as follows:

$$\begin{cases} r_1(t) = q_1(t), \\ r_i(t) = q_i(t) - q_{i-1}(t), \quad \text{for } i = 2, \dots, n. \end{cases} \tag{7}$$

**Table 1**: Twenty-story building model. Mass, stiffness and damping characteristics.

| story | 1–5 | 6–11 | 12–14 | 15–17 | 18–19 | 20 |
|---|---|---|---|---|---|---|
| mass ($\times 10^6$ Kg) | 1.10 | 1.10 | 1.10 | 1.10 | 1.10 | 1.10 |
| stiffness ($\times 10^8$ N/m) | 8.62 | 5.54 | 4.54 | 2.91 | 2.56 | 1.72 |
| relative damping | 2% | | | | | |

By considering the state vector $x(t) = [r_1(t), \dot{r}_1(t), r_2(t), \dot{r}_2(t), \ldots, r_n(t), \dot{r}_n(t)]^T$, we obtain a first-order state-space model

$$\dot{x}(t) = A\,x(t) + B\,u(t) + E\,w(t), \tag{8}$$

with

$$A = \mathcal{C}\,\widehat{A}\,\mathcal{C}^{-1}, \quad B = \mathcal{C}\,\widehat{B}, \quad E = \mathcal{C}\,\widehat{E}, \tag{9}$$

$$\widehat{A} = \begin{bmatrix} [0]_{n\times n} & I_n \\ -M^{-1}K_s & -M^{-1}C_d \end{bmatrix}, \quad \widehat{B} = \begin{bmatrix} [0]_{n\times m} \\ M^{-1}T_u \end{bmatrix}, \quad \widehat{E} = \begin{bmatrix} [0]_{n\times 1} \\ -[1]_{n\times 1} \end{bmatrix}, \tag{10}$$

where $I_n$ is the identity matrix of dimension $n$, $[0]_{n\times m}$ represents a zero-matrix of the indicated dimensions, and $\mathcal{C}$ is the change-of-basis matrix corresponding to the state transformation

$$x(t) = \mathcal{C} \begin{bmatrix} q(t) \\ \dot{q}(t) \end{bmatrix}. \tag{11}$$

In the controller designs and numerical simulations presented in this paper, we consider a twenty-story building model with the mass, stiffness and damping parameters collected in Table 1 [3].

## 3 CONTROLLERS DESIGN

### 3.1 Controllers with full state information

Assuming that the control objective is to reduce the building vibrational response by means of moderate control actions, we consider the controlled-output vector

$$z(t) = C_z\,x(t) + D_z\,u(t), \tag{12}$$

defined by the matrices

$$C_z = \begin{bmatrix} I_{2n} \\ [0]_{m\times 2n} \end{bmatrix}, \quad D_z = \alpha \begin{bmatrix} [0]_{2n\times m} \\ I_m \end{bmatrix}, \tag{13}$$

where $\alpha$ is a scaling factor that can be used to adjust the intensity of the control action. If the full state information is available, we can consider a state-feedback controller $u(t) = Gx(t)$, defined by the state gain matrix $G \in \mathbb{R}^{m\times 2n}$, which produces the closed-loop system

$$\begin{cases} \dot{x}(t) = A_G\,x(t) + Ew(t), \\ z(t) = C_G\,x(t), \end{cases} \tag{14}$$

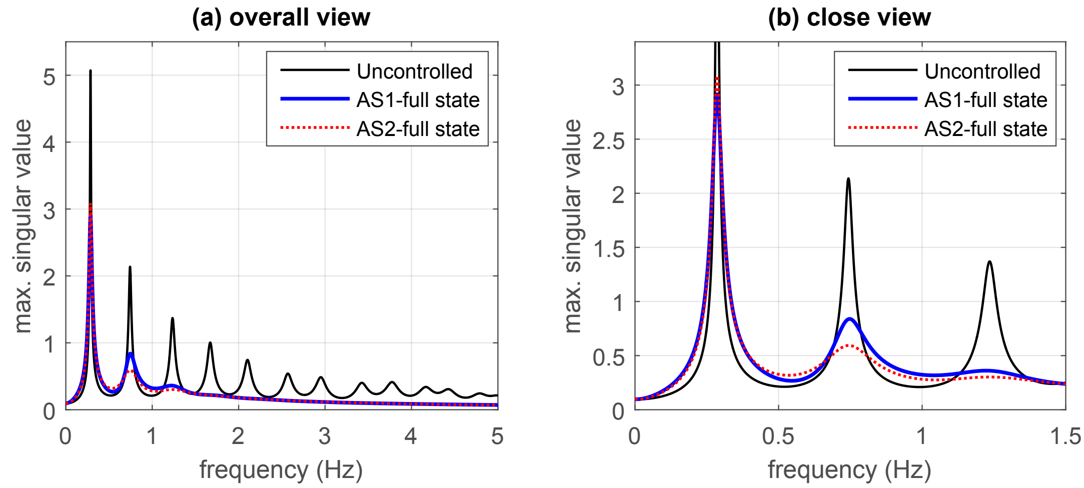


**Figure 2**: Frequency response of the controllers with full state information. Maximum singular values of the closed-loop transfer function $T_{\widetilde{G}_1}(\omega)$ (thick blue solid line), the closed-loop transfer function $T_{\widetilde{G}_2}(\omega)$ (red dotted line) and the open-loop transfer function $T(\omega) = C(2\pi\omega j I_{2n} - A)^{-1}E$ (thin black solid line).

with $A_G = A + BG$ and $C_G = C + DG$. The $H_\infty$ controller design methodology considers the system norm

$$\gamma_G = \sup_{\|w\|_2 \neq 0} \frac{\|z\|_2}{\|w\|_2}, \tag{15}$$

where $\|f\|_2 = \left[\int_0^\infty f^T(t)\, f(t)\, dt\right]^{1/2}$ is the usual continuous 2-norm. The value $\gamma_G$ represents the worst-case gain from the disturbance-input to the closed-loop controlled-output defined by the control gain matrix $G$. The value $\gamma_G$ can be computed by solving the optimization problem

$$\gamma_G = \sup_{\omega} \ \sigma_{\max}\big[T_G(\omega)\big], \tag{16}$$

with

$$T_G(\omega) = C_G(2\pi\omega j I_{2n} - A_G)^{-1}E, \tag{17}$$

where $j = \sqrt{-1}$, $\omega$ is the frequency in hertz, and $\sigma_{\max}[\,\cdot\,]$ denotes the maximum singular value. The controller design objective is obtaining an optimal state-feedback controller $u(t) = \widetilde{G}x(t)$ that produces an asymptotically stable matrix $A_{\widetilde{G}}$ and attains a minimum $H_\infty$-norm value $\gamma_{\widetilde{G}}$. Using an LMI formulation, the optimal state-feedback $H_\infty$ controller can be obtained by solving the following optimization problem [6]:

$$\mathcal{P}: \begin{cases} \text{maximize } \eta \\ \text{subject to } X > 0,\ \eta > 0, \\ \qquad \begin{bmatrix} AX + XA^T + BY + Y^TB^T + \eta EE^T & * \\ C_zX + D_zY & -I_{2n+m} \end{bmatrix} < 0, \end{cases} \tag{18}$$

where $*$ denotes the transpose of the symmetric entry and $X = X^T \in \mathbb{R}^{2n\times 2n}$, $Y \in \mathbb{R}^{m\times 2n}$ are the optimization variables. If an optimal value $\widetilde{\eta}$ is attained in $\mathcal{P}$ for the pair $\big(\widetilde{X}, \widetilde{Y}\big)$, then the

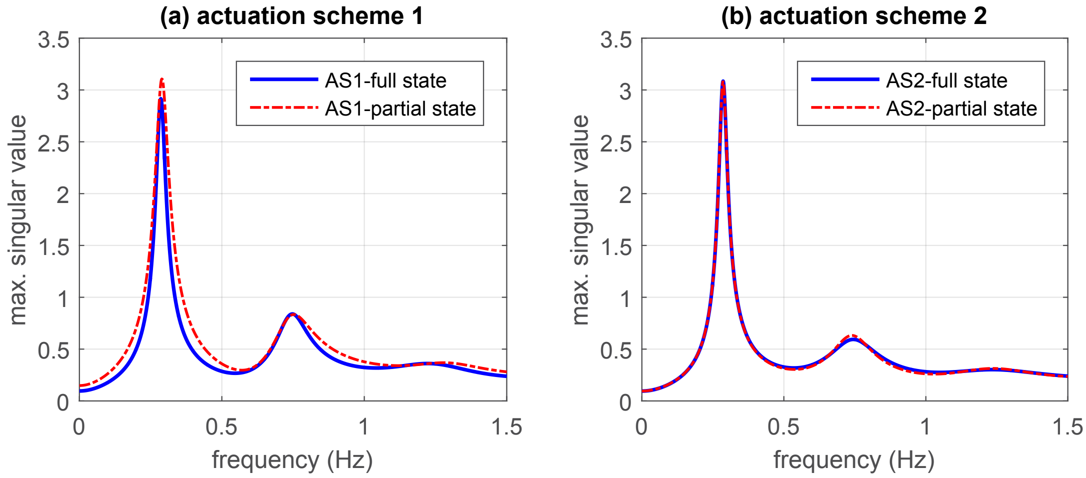


**Figure 3**: Frequency response of the controllers with full and partial state information. (a) Maximum singular values of the closed-loop transfer function $T_{\widetilde{G}_1}(\omega)$ (blue solid line) and the closed-loop transfer function $T_{\widetilde{K}_1}(\omega)$ (red dotted line). (b) Maximum singular values of the closed-loop transfer function $T_{\widetilde{G}_2}(\omega)$ (blue solid line) and the closed-loop transfer function $T_{\widetilde{K}_2}(\omega)$ (red dotted line).

state-feedback gain matrix $\widetilde{G} = \widetilde{Y}\widetilde{X}^{-1}$ is an optimal solution to the $H_\infty$ controller synthesis problem and the corresponding $\gamma$-value can be computed as $\gamma_{\widetilde{G}} = \left(\widetilde{\eta}\right)^{-1/2}$.

To obtain a state-feedback control gain matrix $\widetilde{G}_1$ for the actuation scheme AS1, we solve the LMI optimization problem $\mathcal{P}$ with the values $n = 20$, $m = 10$; the matrices $A$, $B$, $E$ in Eq. (9) corresponding to the values in Table 1 and the control location matrix $T_u^{P_1}$ in Eq. (5); and the controlled-output matrices $C_z$, $D_z$ in Eq. (13) with the scaling factor $\alpha = 10^{-7.4}$. We also compute a state-feedback control gain matrix $\widetilde{G}_2$ for the actuation scheme AS2, using this time the control location matrix $T_u^{P_2}$ in Eq. (6). The $\gamma$-values of the obtained controllers are

$$\gamma_{\widetilde{G}_1} = 2.9153, \ \gamma_{\widetilde{G}_2} = 3.0850, \tag{19}$$

and the corresponding frequency responses are displayed in Fig. 2. Looking at the overall view presented in Fig. 2(a), it can be appreciated that both controllers produce a significant reduction of the building resonant peaks. In accordance with the obtained $\gamma$-values, the plots in Fig. 2(b) show that a slightly higher performance is attained by the actuation scheme AS1 with the controller $\widetilde{G}_1$ in the main resonant peak. However, a better behavior is exhibited by the actuation scheme AS2 with the controller $\widetilde{G}_2$ in the second resonant peak.

### 3.2 Controllers with partial state information

In this section, we assume that the available feedback information is reduced to a vector of measured outputs $y(t) = [y_1(t), y_2(t), \ldots, y_{2m-1}(t), y_{2m}(t)]^T$, where $y_{2i-1}(t) = r_{p_i}(t)$ and $y_{2i}(t) = \dot{r}_{p_i}(t)$ are, respectively, the interstory drift and velocity associated to the interstory actuation device $d_i$ implemented at the building position $p_i$ (between the stories $s_{p_i-1}$ and $s_{p_i}$). Using a measured-output matrix $C_y \in \mathbb{R}^{2m\times 2n}$, the vector $y(t)$ can be written in the form $y(t) = C_y\, x(t)$. For a complete actuation scheme, $C_y$ is an identity matrix of dimension $2n$. For

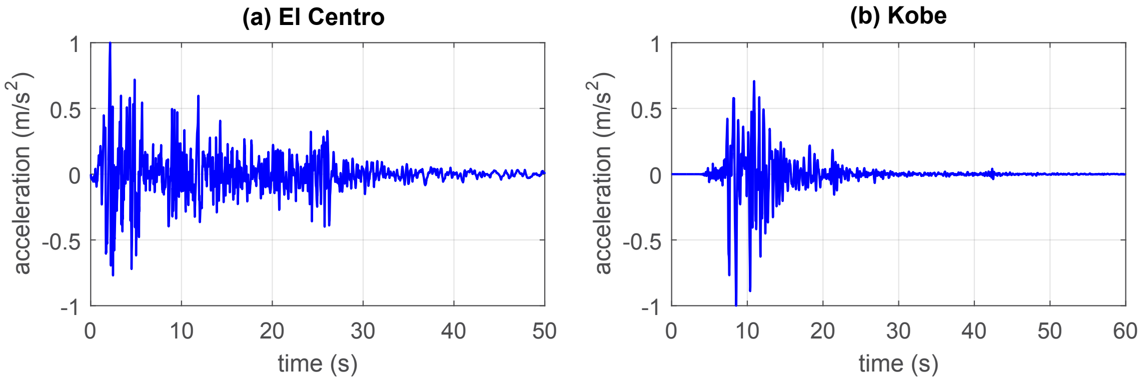


**Figure 4**: Ground acceleration disturbances. (a) North-South El Centro 1940 seismic record scaled to an acceleration peak-value of 1m/s$^2$. (b) North-South Kobe 1995 seismic record scaled to an acceleration peak-value of 1m/s$^2$.

an incomplete actuation scheme defined by a list of positions $P = [p_1, \ldots, p_m]$, the corresponding measured-output matrix $C_y^P$ can be obtained by selecting the rows in positions $2p_i - 1$, $2p_i$ from the identity matrix $I_{2n}$, that is:

$$C_y^P = I_{2n}(2p_1 - 1, 2p_1, \ldots, 2p_m - 1, 2p_m; 1, 2, \ldots, 2n). \tag{20}$$

Thus, for example, the measured-output matrix corresponding to the actuation scheme AS1 is $C_y^{P_1} = \big[I_{20}, [0]_{20\times 20}\big]$. Considering the imposed constraints on the feedback information, we are interested in designing a static output-feedback controller $u(t) = Ky(t)$, defined by a constant output-feedback gain matrix $K \in \mathbb{R}^{m\times 2m}$, that allows computing the vector of control actions from the vector of measured-outputs by means of a simple matrix multiplication. Now, the closed-loop system has the following form:

$$\begin{cases} \dot{x}(t) = A_K\, x(t) + Ew(t), \\ z(t) = C_K\, x(t), \end{cases} \tag{21}$$

with $A_K = A + BKC_y$ and $C_K = C_z + D_zKC_y$, and the associated $H_\infty$-norm takes the value $\gamma_K = \sup_\omega \sigma_{\max}\big[T_K(\omega)\big]$, with $T_K(\omega) = C_K(2\pi\omega j I_{2n} - A_K)^{-1}E$. In this new context, the $H_\infty$ controller design aims at obtaining an optimal static output-feedback controller $u(t) = \widetilde{K}y(t)$ that produces an asymptotically stable closed-loop matrix $A_{\widetilde{K}}$ and, simultaneously, attains a minimum $H_\infty$-norm value $\gamma_{\widetilde{K}}$. The effective computation of this kind of optimal controllers for large-scale systems is a very difficult problem that still remains unsolved. However, according to the results presented in [7, 8], a suboptimal static output-feedback $H_\infty$ controller can be designed by solving the following LMI optimization problem:

$$\mathcal{P}_o : \begin{cases} \text{maximize } \eta \\ \text{subject to } X_Q > 0,\ X_R > 0,\ \eta > 0 \text{ and the LMI in (23)}, \end{cases} \tag{22}$$

$$\begin{bmatrix} AQX_QQ^T + QX_QQ^TA^T + ARX_RR^T + RX_RR^TA^T + BY_RR^T + RY_R^TB^T + \eta EE^T & * \\ C_zQX_QQ^T + C_zRX_RR^T + D_zY_RR^T & -I_{2n+m} \end{bmatrix} < 0, \tag{23}$$

where $*$ denotes the transpose of the symmetric entry, $X_Q$, $X_R$ and $Y_R$ are the optimization variables, $Q$ is a matrix whose columns contain a basis of $\mathrm{Ker}(C_y)$, and the matrix $R$ has the form $R = C_y^\dagger + QQ^\dagger \widetilde{X} C_y^T \big(C_y \widetilde{X} C_y^T\big)^{-1}$, where $C_y^\dagger = C_y^T \big(C_y C_y^T\big)^{-1}$ and $Q^\dagger = \big(Q^T Q\big)^{-1} Q^T$ are the *Moore-Penrose* pseudoinverses of $C_y$ and $Q$, respectively, and $\widetilde{X}$ is the optimal $X$-matrix obtained in the LMI optimization problem $\mathcal{P}$ corresponding to the state-feedback design. If an optimal value $\widetilde{\eta}_{\mathrm{o}}$ is attained in $\mathcal{P}_{\mathrm{o}}$ for the triplet $\big(\widetilde{X}_Q, \widetilde{X}_R, \widetilde{Y}_R\big)$, then the matrix $\widetilde{K} = \widetilde{Y}_R \big(\widetilde{X}_R\big)^{-1}$ defines a static output-feedback controller $u(t) = \widetilde{K} y(t)$ with asymptotically stable closed-loop matrix $A_{\widetilde{K}}$, and the value $\widetilde{\gamma}_{\widetilde{K}} = \big(\widetilde{\eta}_{\mathrm{o}}\big)^{-1/2}$ provides an upper bound of the associated $H_\infty$-norm value $\gamma_{\widetilde{K}}$.

To design a partial-state controller for the proposed twenty-story building model with the actuation scheme AS1, we consider the measured-output vector

$$y^{(1)}(t) = [r_1(t), \dot{r}_1(t), r_2(t), \dot{r}_2(t), \ldots, r_{10}(t), \dot{r}_{10}(t)]^T, \tag{24}$$

and solve the LMI optimization problem $\mathcal{P}_{\mathrm{o}}$ in Eq. (22) with the same matrices $A$, $B$, $E$, $C_z$ and $D_z$ used in the design of the state-feedback gain matrix $\widetilde{G}_1$, and the matrices $Q$, $R$ defined by the measured-output matrix $C_y^{P_1} = \big[I_{20}, [0]_{20\times 20}\big]$ and the optimal $X$-matrix computed in the associated full-state controller design. As a result, we obtain an output-feedback gain matrix $\widetilde{K}_1$ with a $\gamma$-value upper bound $\widetilde{\gamma}_{\widetilde{K}_1} = 3.3846$. The frequency response of the partial-state controller $u(t) = \widetilde{K}_1 y^{(1)}(t)$ and the associated full-state controller $u(t) = \widetilde{G}_1 x(t)$ are displayed in Fig. 3(a). The plots in the figure show a small (but clearly appreciable) loss of performance of the partial-state controller (red dash-dotted line) with respect to the full-state controller (blue solid line). Using the closed-loop transfer function $T_{\widetilde{K}_1}(\omega)$, we obtain that the actual $\gamma$-value of the partial-state controller is $\gamma_{\widetilde{K}_1} = 3.1072$, which represents an increment of 6.58% with respect to the optimal value $\gamma_{\widetilde{G}_1} = 2.9153$.

For the distributed actuation scheme AS2, the vector of measured outputs $y^{(2)}(t)$ contains the interstory drifts and velocities indicated in the list of positions $P_2 = [1, 2, 3, 4, 5, 7, 10, 13, 16, 19]$. In this case, we obtain an output-feedback gain matrix $\widetilde{K}_2$ with a $\gamma$-value upper bound $\widetilde{\gamma}_{\widetilde{K}_2} = 3.0857$ by solving the LMI optimization problem $\mathcal{P}_{\mathrm{o}}$ with the same matrices $A$, $B$, $E$, $C_z$ and $D_z$ used in the design of the state-feedback gain matrix $\widetilde{G}_2$, and the matrices $Q$ and $R$ defined by the measured-output matrix $C_y^{P_2}$ and the corresponding auxiliary $X$-matrix. Comparing the value of the upper bound $\widetilde{\gamma}_{\widetilde{K}_2}$ with the optimal value $\gamma_{\widetilde{G}_2} = 3.0850$, it can be seen that the static output-feedback controller $u(t) = \widetilde{K}_2 y^{(2)}(t)$ is practically optimal. In fact, the plots presented in Fig. 3(b) show that the frequency response of the partial-state controller defined by the output-feedback gain matrix $\widetilde{K}_2$ (red dash-dotted line) is practically equal to the frequency response of the optimal full-state controller defined by the state-feedback gain matrix $\widetilde{G}_2$ (blue solid line).

## 4 NUMERICAL RESULTS

To further illustrate the behavior of the proposed partial-state controllers, a suitable set of numerical simulations has been carried out using the scaled North-South components of El Centro 1940 and Kobe 1995 seismic records as ground acceleration inputs (see Fig. 4). For the El Centro seismic disturbance, the absolute peak-values of the interstory-drifts, the story absolute

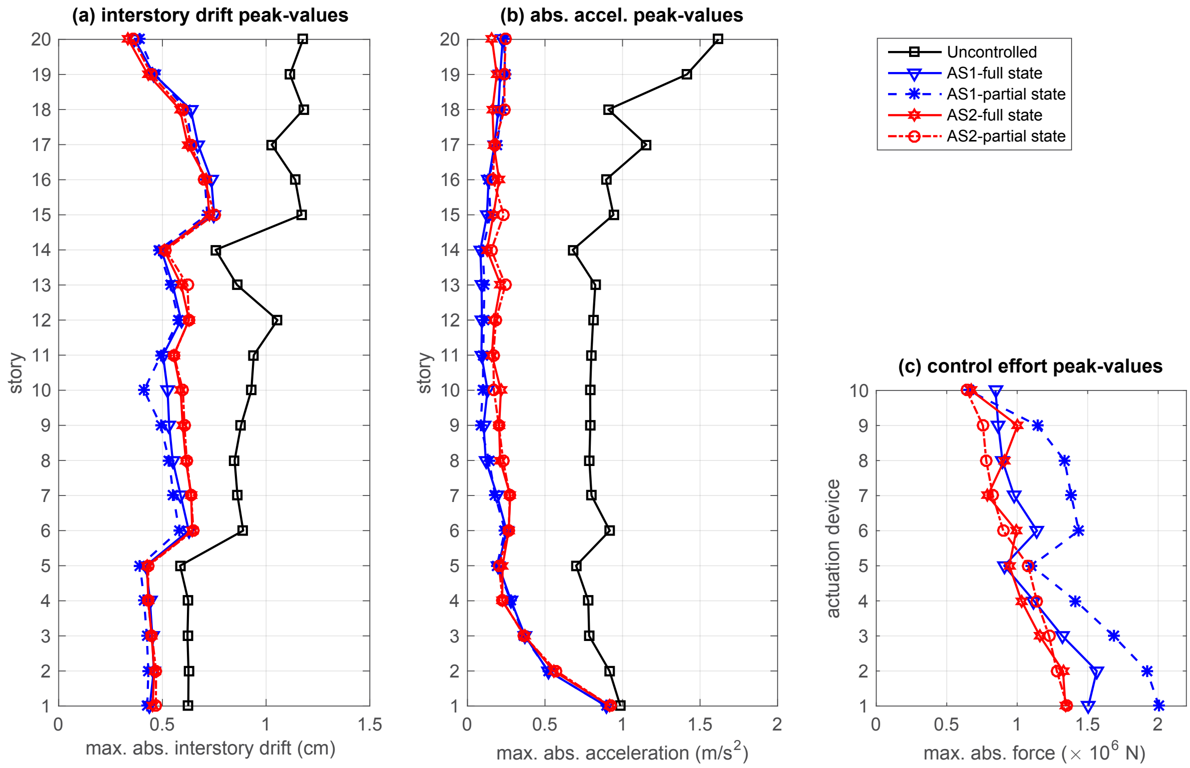


**Figure 5**: Response of the twenty-story building model corresponding to the scaled North-South El Centro 1940 seismic record for the uncontrolled configuration (black line with squares), the actuation scheme AS1 with the full-state controller defined by the state-feedback gain matrix $\widetilde{G}_1$ (blue solid line with triangles), the actuation scheme AS1 with the partial-state controller defined by the output-feedback gain matrix $\widetilde{K}_1$ (blue dashed line with asterisks), the actuation scheme AS2 with the full-state controller defined by the state-feedback gain matrix $\widetilde{G}_2$ (red solid line with hexagrams), and the actuation scheme AS2 with the partial-state controller defined by the output-feedback gain matrix $\widetilde{K}_2$ (red dash-dotted line with circles). (a) Interstory drift peak-values. (b) Absolute acceleration peak-values. (c) Control effort peak-values.

accelerations and the actuation control efforts corresponding to the different control configurations are presented in Fig. 5, where the black lines present the response of the uncontrolled building, the blue lines correspond to the controllers of the actuation scheme AS1, and the red lines represent the controllers of the distributed actuation scheme AS2. Also, solid lines are used for the full-state controllers and discontinuous lines for the partial-state controllers. Looking at the plots in the figure, the following facts can be appreciated: (i) All the proposed controllers provide a good level of reduction in the interstory drift and absolute acceleration peak-values with respect to the uncontrolled response. (ii) For the distributed actuation control scheme AS2, the behavior of the full-state controller and the partial-state controller (red lines) are very similar. (iii) For the concentrated actuation scheme AS1, the interstory drift peak-values produced by the partial-partial state controller (blue dashed line with asterisks) are slightly smaller that those attained by the full-state controller controller (blue solid line with triangles). However,

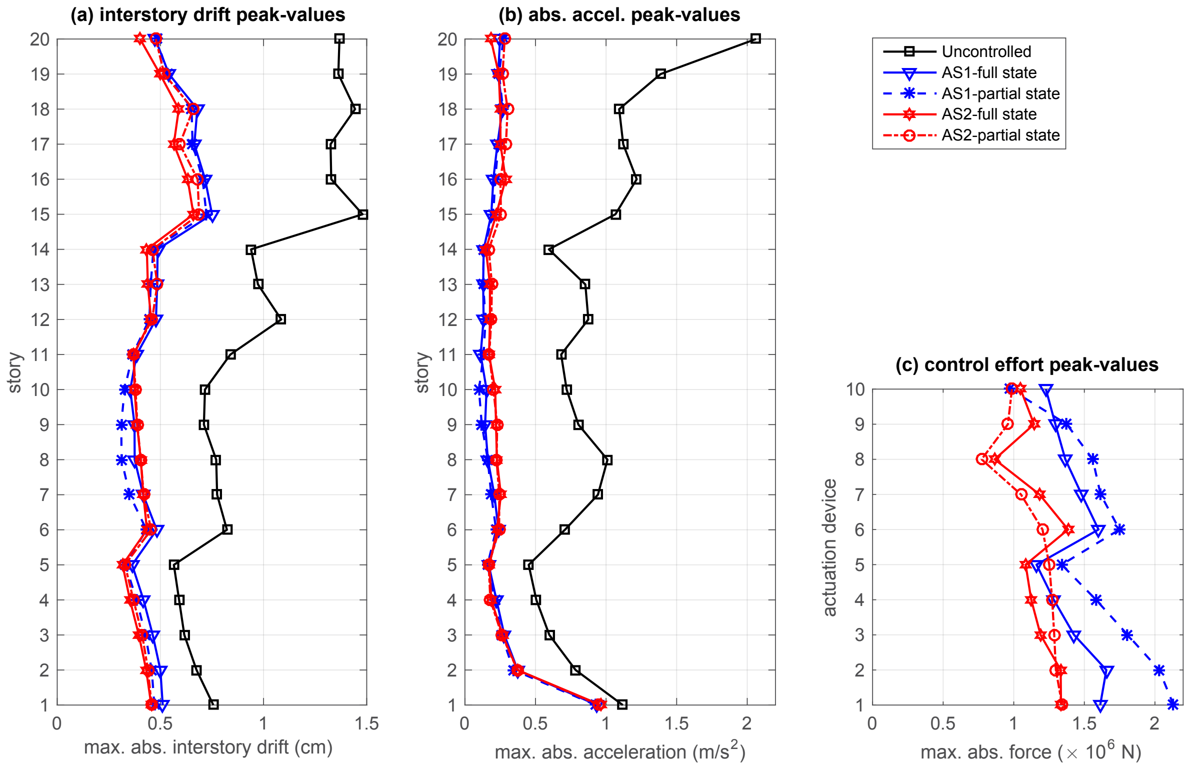


**Figure 6**: Response of the twenty-story building model corresponding to the scaled North-South Kobe 1995 seismic record for the uncontrolled configuration (black line with squares), the actuation scheme AS1 with the full-state controller defined by the state-feedback gain matrix $\widetilde{G}_1$ (blue solid line with triangles), the actuation scheme AS1 with the partial-state controller defined by the output-feedback gain matrix $\widetilde{K}_1$ (blue dashed line with asterisks), the actuation scheme AS2 with the full-state controller defined by the state-feedback gain matrix $\widetilde{G}_2$ (red solid line with hexagrams), and the actuation scheme AS2 with the partial-state controller defined by the output-feedback gain matrix $\widetilde{K}_2$ (red dash-dotted line with circles). (a) Interstory drift peak-values. (b) Absolute acceleration peak-values. (c) Control effort peak-values.

significantly larger control-effort peak-values are also required by the partial-state controller. Looking at the graphics in Fig. 6, the same facts can be appreciated in the peak-value plots obtained for the Kobe seismic disturbance. These time-response results are entirely consistent with the frequency-response characteristics observed in Section 3, and indicate that a similar performance level is attained by the full-state controllers in both actuation schemes. For the partial-state controllers, the situation is clearly different. In the distributed actuation scheme AS2, the partial-state controller is not affected by the reduced feedback information, and it attains practically the same level of performance as the full-state controller. In contrast, an evident loss of effectiveness can be observed in the partial-state controller corresponding to the concentrated actuation scheme AS1.

*Remark.* All the computations in this paper have been carried out using Matlab© R2015b on a regular laptop with an Intel© Core™ i7-2640M processor at 2.80 GHz. The LMI optimization problems have been solved with the function `mincx()` included in the Robust Control Toolbox™.

## 5 CONCLUSIONS AND FUTURE DIRECTIONS

In this paper, the design of partial-state controllers with incomplete multi-actuation systems for the seismic protection of large buildings has been investigated. The proposed approach considers a partially instrumented building with a system of interstory force-actuation devices implemented at selected levels of the building, and an associated set of collocated sensors that provide the interstory drifts and velocities corresponding to the instrumented stories. Using a static output-feedback $H_\infty$ controller design methodology, partial-state controllers have been designed for a twenty-story building with two different actuation schemes, and the corresponding frequency and time responses have been investigated. The obtained results confirm the effectiveness of the proposed partial-state controllers and indicate that a suitable distribution of the instrumented stories is a relevant factor in the control system design. After these positive outcomes, further research effort should be invested in finding a suitable methodology to determine the optimal configuration of distributed multi-actuation systems with partial state information. This is certainly an important and challenging problem, specially for large-scale structures.

### Acknowledgments

This work was partially supported by the Spanish Ministry of Economy and Competitiveness under Grant DPI2015-64170-R/FEDER.

## REFERENCES

[1] Spencer, B.F. and Nagarajaiah, S. State of the art of structural control, *Journal of Structural Engineering* (2003) **129**:845–856.

[2] Thenozhi, S. and Yu, W. Advances in modeling and vibration control of building structures, *Annual Reviews in Control* (2013) **37**:346–364.

[3] Wang, Y., Lynch, J.P. and Law, K.H. Decentralized $H_\infty$ controller design for large-scale civil structures, *Earthquake Engineering and Structural Dynamics* (2009) **38**:377–401.

[4] Palacios-Quiñonero, F., Rubió-Massegú, J., Rossell, J.M. and Karimi, H.R. Vibration control strategy for large-scale structures with incomplete multi-actuator system and neighbouring state information, *IET Control Theory and Applications* (2016) **10**:407–416.

[5] Chopra, A.K. *Dynamics of Structures. Theory and Applications to Earthquake Engineering 3rd ed.* Prentice Hall (2007).

[6] Boyd, S., Ghaoui, L.E., Feron, E. and Balakrishnan, V. *Linear Matrix Inequalities in System and Control Theory.* SIAM Studies in Applied Mathematics (1994).

[7] Rubió-Massegú, J., Rossell, J.M., Karimi, H.R. and Palacios-Quiñonero, F. Static output-feedback control under information structure constraints, *Automatica* (2013) **49**:313–316.

[8] Palacios-Quiñonero, F., Rubió-Massegú, J., Rossell, J.M. and Karimi H.R. Feasibility issues in static output-feedback controller design with application to structural vibration control. *Journal of the Franklin Institute* (2014) **351**:139–155.